Journal of Radiation and Nuclear Applications
An International Journal

http://dx.doi.org/10.18576/jrna/090209

Radiation Shielding Properties of Mono and Polycrystalline Solar Cells

Ghsson Ali Al-zaidi[1], *H. A. Saudi*[1*], *Ibrahim A. Nassar*[2], *Kamilia Sedeek*[1]

[1]Department of Physics, Faculty of Science, Al-Azhar University (Girls' Branch), Cairo, Egypt.
[2]Department of Electricity, Faculty of Engineering, Al-Azhar University, Cairo, Egypt.

Received: 2 Feb. 2024, Revised: 22 March. 2024, Accepted: 1 April. 2024.
Published online: 1 May 2024

Abstract: This study focuses on the radiation-shielding characteristics of Monocrystalline and Polycrystalline solar cells. Mass attenuation coefficient (μ/ρ) values of the solar cells have been calculated using Win X-Com and GEANT4 code at various photon energies ranging from 80 to 2614 keV and compared to those of experimental results. The obtained results exhibited that experimental and calculated are in good agreement at all energies. Some shielding parameters such as effective atomic number (Zeff), effective electron density (Nel), half value layer (HVL), and mean free path (MFP). Moreover, macroscopic effective removal cross sections (ΣR) for fast neutrons have been evaluated. It can be concluded that photovoltaic systems are superior shielding materials for both gamma rays and neutrons.
Keywords: Radiation Shielding, effective atomic number, macroscopic effective removal cross-sections.

1 Introduction

Electromagnetic waves such as X-rays and gamma rays are already known to produce energy that travels at the speed of light. X-rays, gamma rays, and neutrons are examples of ionizing radiation that are dangerous to the cells and tissues of living organisms. Long-term exposure to ionizing radiation can lead to many diseases, genetic changes, cancer, and even death [1]. Therefore, it is essential to develop radiation shielding products to defend against these dangerous rays. Activities such as the medical uses of radiation, the operation of nuclear installations, the production, transport, and use of radioactive material, and the management of radioactive waste must therefore be subject to standards of safety. There are three safety parameters namely: time, distance, and shielding. The radiation exposure can be controlled to some extent by spending minimum time and by keeping a maximum distance from the radiation source. The third parameter shielding, plays an essential role in radiation physics and is a controllable parameter.

Due to flexibility in this parameter and liberty for choice of material, radiation science workers are searching for better γ−rays protecting materials for their effective use in different applications. As a result, a suitable shielding material is required to protect live beings and minimize radiation levels from nuclear power plants, industries, research laboratories, and medical departments [2-4]. Concretes have successfully attenuated alpha, beta, neutron beams, X-rays, and gamma rays in radiation therapy facilities, reactors, and nuclear waste storage sites. So, in an environment of high radiation exposure, concrete is used as a radiation shielding material because it is cheap, and it can be molded easily into any desired design.

It was usual to absorb ionizing radiation by using concrete of all kinds or various glass systems in previous research [5–10] but what is new in this work is to:

1- prove that the solar cells have a dual function, generating photovoltaic energy and absorbing ionizing radiation. For this purpose, mono-crystalline and polycrystalline Si solar cells have been used. Linear attenuation coefficients and some shielding parameters have been calculated.

2- A comparison between mono-crystalline and polycrystalline cells has been made.

Recently Solar technologies for the development and exploration of environmentally friendly energy Sources is becoming an urgent topic to avoid many catastrophic consequences. Photovoltaic (PV) setups (Panel/array) have been employed for solar energy Conversion. Photovoltaic materials are Semiconductors chosen according to efficiency and cost. The most widely used is Monocrystalline (Si) with high efficiency and

*Corresponding author e-mail: heba_saudi@azhar.edu.eg

polycrystalline (Si) with lower efficiency but having a lower cost/watt. As Solar Panels Cover millions of meters square all over the world and are exposed to all kinds of ionizing and non-ionizing radiation, we intended in this work to study the PV solar cell in addition to energy conversing in absorbing ionizing radiation. Measurements of the absorption Coefficient and the calculation of the linear attenuation coefficient and some other shielding parameters have been carried out. A comparison between Monocrystalline and Polycrystalline solar cells has also been made.

2 Theoretical calculations:

This section provides a summary of the theoretical relationships used in the current work. According to the Lambert-Beer law, a collimated mono-energetic gamma-ray beam attenuates in matter [11,12]

$$I=Io\ e^{-\mu t} \qquad (1)$$

Where I0 is the gamma ray's initial intensity, I is its intensity following attenuation through a material of thickness t (cm), and is the material's linear attenuation coefficient μ(cm-1). The material's mass attenuation coefficient (μm) is calculated by dividing by the density of the material (ρ). For a chemical or combination, the mass attenuation coefficient [13,14] is given by:

$$\mu m= \sum wi\ (\mu m)i \qquad (2)$$

Where wi and (μm)i are the ith constituent element's weight fraction and mass attenuation coefficient, respectively. The thickness of the material that reduces the photon beam intensity to half of its original value (I0), i.e. (½) I0, is called the half value layer (HVL) and is given by:

$$HVL = Ln\ 2 /\mu \qquad (3)$$

Where μ is the linear attenuation coefficient of the material at a given photon energy. The following formula can be used to get the total atomic cross section (σt,a) for any molecule using the information of the mass attenuation coefficient ;

$$\sigma t,a= \mu m\ N/NA \qquad (4)$$

Where NA is Avogadro's number and N is the atomic mass of materials. Similarly, the total electronic cross section (σ t,e) is given by [15, 16]

$$\sigma t,e=(1/ NA)\Sigma i(fiAi/Zi)(\ \mu/\rho), \qquad (5)$$

Where fi denotes the fractional abundance of the element i concerning the number of atoms such that f1 + f2 + f3 + . . . + fi =1, Zi is the atomic number of ith elements. Finally, by using Eqs. (4) and (5), the effective atomic number (Zeff) can be defined as [17]

$$Zeff = \sigma t,a / \sigma t,e \qquad (6)$$

3 Experimental Section

Si solar cells for shielding examinations, monocrystalline (JS158M5) and polycrystalline (LWP5BB-157) solar cells (3 of each) have been used as shown in figure 1. The density (ρ) of the cell was measured using the Archimedes method and using toluene as an immersed liquid at room temperature. The density (ρ) was calculated according to the formula:

$$\rho= Wa/ \{Wa- Wb\} \times \rho L \qquad (7)$$

Where Wa and Wb are the weight of the sample in air and toluene, respectively. ρL is density of toluene (0.866 g /cm3).

For investigation of the solar cells' hardness (Hv), The cell was indented using a Vicker's diamond indentor. A light weight of 10 g was applied to the cell. Ten indentations in each of the chosen villages were treated with each sample. Errors in the measured values were roughly 3%, according to the standard deviation. The diagonal lengths were calibrated. Hv is calculated by the following equation [19]:

$$H = (1.8544\ P)/d2 \qquad (8)$$

Where F is in Kg f, P is the indentation load in gm, and d is the average diagonal length impression produced by the indenter in milli meter [18,19].

Using a NaI (Tl) 2 × 2 scintillation detector, the gamma-ray absorption was measured and the NaI (TI) detector was surrounded with 5 mm lead (collimation detector), to prevent the scattered γ-rays from reaching the detector. Radioactive sources used for the measurement are Ba-133, Co-60, Cs-137, and Th-232 with activities 5.3, 4.9, 9.5, and 8.6 μCi respectively; Each was used at different photon energies. The energy spectrum of gamma rays emitted from 4 sources is given in Figure (2, a-d (. Incident and transmitted intensities of photons were measured on (MCA) for a fixed preset time for each sample by selecting a narrow region symmetrical concerning the centroid of the photo peak. Counting time was chosen such that 103–105 counts were recorded under each photo peak. Calculated values of the mass attenuation coefficient for each sample mixture were calculated by WinXCom computer program (version 3.1) based on the mixture rule and Geant4-based Monte Carlo simulations. Figure (3) shows the arrangement system used in this experiment.

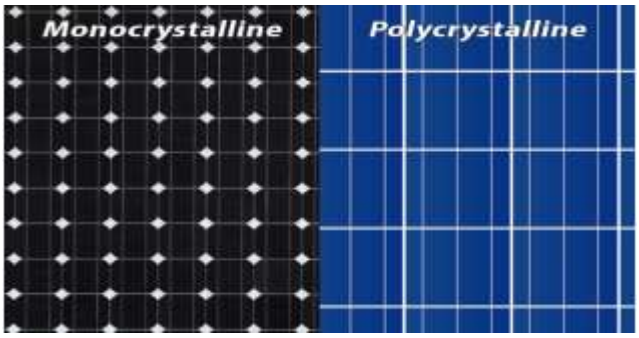

Fig.1: Monocrystalline and Polycrystalline solar cells used for shielding examinations.

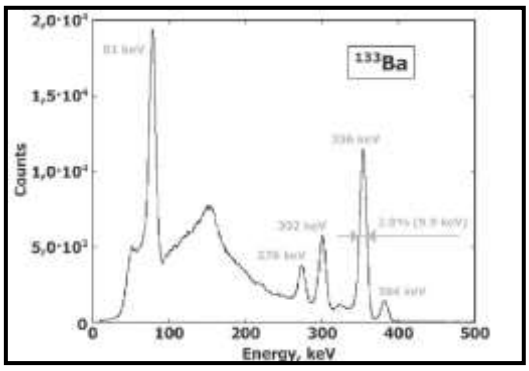

(a)

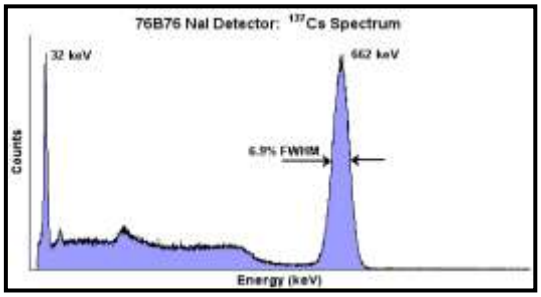

(b)

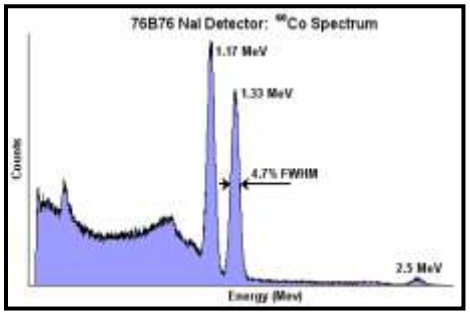

(c)

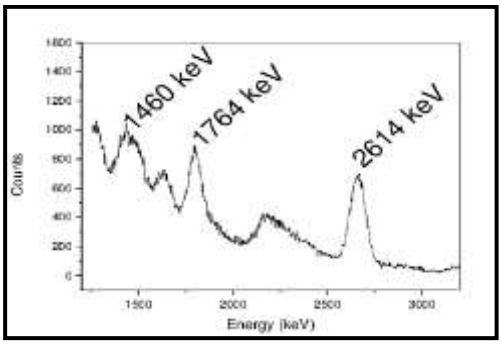

(d)

Fig.2: Spectrum of gamma-ray sources for (a) ^{133}Ba, (b) ^{137}Cs, (c) ^{60}Co, and (d) ^{232}Th.

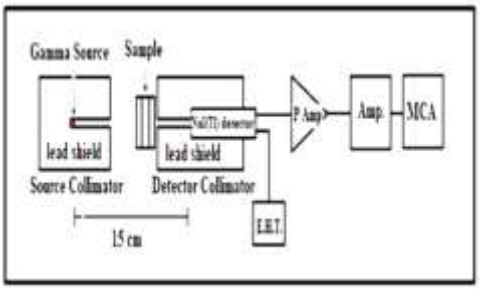

Fig.3: Experimental setup technique for gamma-ray detection.

4 Results and discussions

The value of the measured density and microhardness of the studied mono and polycrystalline Si solar cells are given in Table 1.

Solar cells consist of a high percentage of silicon, which is a tetravalent metal and a solid crystalline substance. The yield strength of cells is an important parameter when designing. The higher the yield stress, the stronger the material. Semiconductors have high yield stress because they resist bending under stress. The cells have a relatively small Vickers hardness at load 10 g and time 10 sc. These tests are important in the solar cell industry because stiffness determines the cells' ability to cut into thin layers [19]. The two cells are very close to each other in the value of hardness and the change between them is within the limits of error as seen in Table 1.

To study Gamma, X-ray, and fast neutron attenuation capabilities as a function of thickness, single, two, and three cells were used respectively to give 0.2 mm, 0.4 mm, and 0.6 mm in thickness. Figures 4 and 5 give the plot of ln I / Io versus the thickness at different energies. The slope has been calculated to find out the linear attenuation coefficient

of each at different energies as shown in figure 6. Knowing the practically measured density and the linear attenuation coefficient, the mass attenuation coefficient can be calculated according to relation 2. Mass attenuation coefficients (μm) for mono and poly solar cells obtained from experimental gamma measurements. Theoretical calculation of the mass attenuation coefficients (μm) has been employed using Win X-Com and Geant4 code programs for mono and polycrystalline Si solar cells. Table 2 shows a comparison between experimental and theoretical values. The great agreement can be detected.

According to Table 2, it is seen that the μm values are higher in the low energy level and then tend to decrease rapidly with increasing energy. Bashter et al [20] attributed this rapid decline to the predominance of the photovoltaic effect in the low-energy region [20]. In this region, the cross-section of the interaction of photons with material changes depending on Z4-5/E3,5[21]. However, photons are completely absorbed or lose their energy to a large extent. It is to be noted that the decrease of the μm values is slower at the average energy range. This is probability due to the dominance of Compton scattering over this energy and the change of the Compton cross-section with Z/E [22-24]. Table 2 also that the photon absorption capacity of polycrystalline solar cells is higher than that of mono-crystalline solar ones.

The energy-dependent change Half-value layer (HVL) for different solar cells has been calculated and given in Figure 7. As shown in Figure 7 the HVL values rise rapidly especially at medium energies as the photon energy goes up. This may be attributed to the increase in the number of secondary photons with the Compton effect that dominates in the middle energy region. For this reason, thicker cells are needed for these energies. It is recommended to have a low HVL value for good protection. The HVL values are indicated for the polycrystalline type of solar cells smaller than those in the mono-crystalline type. HVL is related to another quantity called the mean free path (MFP), which describes the average distance a photon travels in the medium before an interaction occurs. MFP, which is the reciprocal of the linear attenuation coefficient, can be calculated and is shown in Figure 8. Figure 8 indicates the MFP of the different solar cells, which increase with the increase in energy. It is also clearly noted that the HVL and MFP of the solar cells are close as in Figures 7 and 8, and this is attributed to the slight difference in density. Figure 8 also shows that polycrystalline solar cells have better shielding properties than mono-crystalline cells since they have lower MFP values, which indicates the possibility of using polycrystalline solar cells as radiation shielding materials. Zeff and Ne values for the solar cells in Fig. 9 and 10. Zeff takes on its largest values at lower energies. Large values of Zeff are due to the cross-section of the photo electrochemical reaction to Z4-5 decreases of Zeff values. Fast speeds at medium energies where the Compton Effect is dominant, Zeff values for the solar cells. They are very close to each other. It is seen that Zeff values go up in polycrystalline cells. The change of Ne values with photon energy is like Zeff. Polycrystalline cells have increased attenuation of X-rays and gamma rays. It can be pointed out that multiple and more popular polycrystalline solar cells are more prosperous in absorbing X-rays.

The removal of the effective macroscopic cross-section (∑R) is the probability that the fission energy is fast. The neutron beam penetrates matter and causes a collision [23-25]. This parameter can be calculated from the Win X-com software [26, 27]. Polycrystalline solar cells have a higher ΣR value as shown in Table 1 than Monocrystalline solar cells. In general, based on these results, the solar cells show perfect shielding vs comparison of neutron and photon radiation. We believe that the results obtained from this study will serve as a guide in producing new Polycrystalline, lighter, and economical poly-type solar cells.

Table 1: The density and the effective removal macroscopic cross-section of the solar cells

	Monocrystalline	**polycrystalline**
ρ (g/cm^3)	2.32	2.47
Micro hardness (kg/mm^2)	450±28	475±31
ΣR (cm^{-1})	0.08927	0.09886

Table 2: Mass attenuation coefficients (cm^2/g) obtained by using the experimental and theoretical method of mono and polycrystalline versus photon energy.

E (KeV)	80	238	356	662	1173	1333	2614
Mono Exp.	0.8392	0.1972	0.1571	0.11602	0.08703	0.08202	0.0581
poly Exp.	1.8012	0.2811	0.1862	0.1231	0.0902	0.08303	0.0601
Mono Win X-Com	0.8931	0.2104	0.16902	0.1272	0.0921	0.0846	0.0637
Poly Win X-Com	1.861	0.2941	0.19803	0.1281	0.0932	0.0887	0.0612
Mono Geant4	0.8791	0.2073	0.1621	0.1193	0.0886	0.0829	0.0605
Poly Geant4	1.848	0.2861	0.1892	0.1251	0.0928	0.0843	0.0604

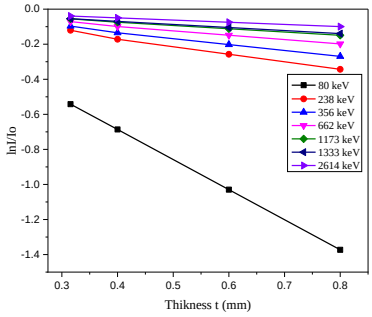

Fig. 4: Plot of I_0/I Vs thickness t (mm)for monocrystalline at different energies (KeV).

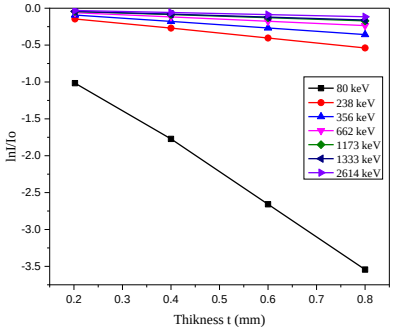

Fig. 5: Plot of I_0/I Vs thickness t (mm) for polycrystalline at different energies (KeV).

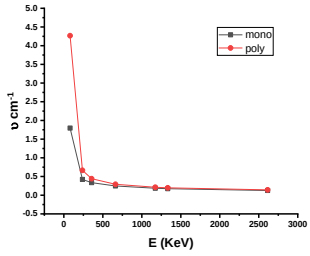

Fig. 6. Linear attenuation coefficients (cm^{-1}) of mono and poly crystalline versus photon energy

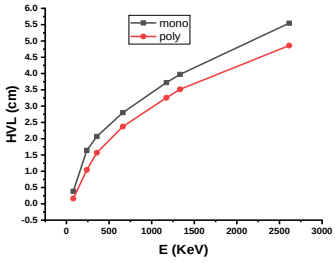

Fig. 7. **Half**-value layer (HVL) (cm) of mono and poly crystalline versus photon energy

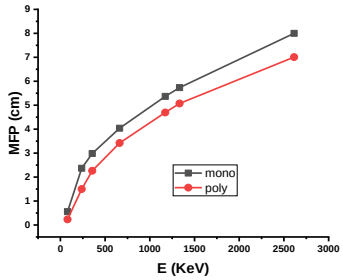

Fig. 8. Mean free path (MFP) (cm) of mono and polycrystalline versus photon energy.

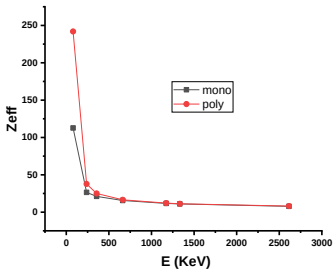

Fig. 9. Effective atomic number of mono and polycrystalline with photon

energy (MeV)

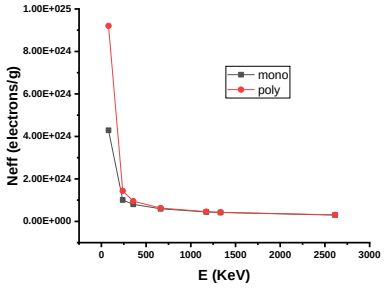

Fig. 10. Electron density values of mono and polycrystalline with photon

energy (MeV).

4 Conclusions

In the present work, the extent to which different solar cells absorb ionizing radiation was studied. Different thicknesses have been investigated. Experimental studies were conducted by measuring the density of different solar cells and the absorption of gamma rays at different energies. um values were calculated experimentally and theoretically. It is proved that the experimental and theoretical um values agree with each other, and the calculated error is in the range of 0.001-0.044. It was found that the polycrystalline-type cells have the highest um value. Zeff and Ne, while the HVL values of these cells are the smallest. Finally, equivalent, and microscopic dose absorption rates. To accelerate the calculated neutrons Poly solar cells, have the highest ΣR value. In general, neutron-reduction polycrystalline solar cells have higher capacities. Based on

these results, poly-type solar cells show perfect neutron and photon shielding. From the foregoing, it is clear that polycrystalline solar cells are a new production in shielding, lighter in weight, and cheaper in economic terms.

Declarations

Ethical Approval: Authors declare that this manuscript is original, has not been published before, and is not currently being considered for publication elsewhere.

Consent to participate: Not applicable.

Consent to publish: Not applicable.

Conflict of interest: The authors declare that they have no conflict of interest.

Authors' contributions: H. A. Saudi, and Ghsson Ali Al-zaidi: wrote the main manuscript text; Ibrahim A. Nassar prepared and drew all figures; Kamilia Sedeek reviewed and revised the manuscript.

Competing interests: The authors declare no competing interests.

Data availability: All data generated or analyzed during this study are included in this publication.

References

[1] T. Kaur, J. Sharma, T. Singh, Review on the scope of metallic alloys in gamma rays shield designing, Prog. Nucl. Energy. 113 (2019). https://doi.org/10.1016/j.pnucene.2019.01.016.

[2] W.M. Abd-Allah, H.A. Saudi, K.S. Shaaban, H.A. Farroh, Investigation of structural and radiation shielding properties of 40B2O3–30PbO–(30-x) BaO-x ZnO glass system, Appl. Phys. A. 125 (2019) 275. https://doi.org/10.1007/s00339-019-2574-0.

[3] G. Lakshminarayana, M.G. Dong, A. Kumar, Y. Elmahroug, A. Wagh, D.E. Lee, J. Yoon, T. Park, Assessment of gamma-rays and fast neutron beam attenuation features of Er2O3-doped B2O3–ZnO–Bi2O3 glasses using XCOM and simulation codes (MCNP5 and Geant4), Appl. Phys. A Mater. Sci. Process. 125 (2019) 1–14. https://doi.org/10.1007/s00339-019-3099-2.

[4] A.M. El-Khayatt, H.A. Saudi, Recycling of waste porcelain into newly developed bismo-borate glass admixture with Gd3+ ions for nuclear radiation protection uses: An experimental and theoretical study, Radiat. Phys. Chem. 203 (2023) 110612. https://doi.org/10.1016/j.radphyschem.2022.110612.

[5] P. Sikora, A.M. El-Khayatt, H.A. Saudi, M. Liard, D. Lootens, S.-Y. Chung, P. Woliński, M. Abd Elrahman, Rheological, Mechanical, Microstructural and Radiation Shielding Properties of Cement Pastes Containing Magnetite (Fe3O4) Nanoparticles, Int. J. Concr. Struct. Mater. 17 (2023). https://doi.org/10.1186/s40069-022-00568-y.

[6] H.M. Gomaa, H.A. Saudi, I.S. Yahia, H.Y. Zahran, B.M.A. Makram, Effect of Y2O3 Content on the Structural, Optical, and Shielding Properties of the Ca/Na Lead Borovanadate Multi-Component Oxide Glass, J. Inorg. Organomet. Polym. Mater. (2023). https://doi.org/10.1007/s10904-023-02549-4.

[7] H.M.H. Zakaly, D.E. Abulyazied, S.A.M. Issa, A.W. Alrowaily, H.A. Saudi, H.M. Abomostafa, Optical, Microhardness, and Radiation Shielding Properties of Rare Earth Doped Strontium Barium Titanate Polyvinylidene Fluoride Nanocomposites, J. Inorg. Organomet. Polym. Mater. (2023). https://doi.org/10.1007/s10904-023-02564-5.

[8] D.E. Abulyazied, S.A.M. Issa, A.W. Alrowaily, H.A. Saudi, H.M.H. Zakaly, E.S. Ali, Polylactic acid tungsten trioxide reinforced composites: A study of their thermal, optical, and gamma radiation attenuation performance, Radiat. Phys. Chem. 205 (2023) 110705. https://doi.org/10.1016/j.radphyschem.2022.110705.

[9] J.M. An, H. Lin, E.Y.B. Pun, D.S. Li, Synthesis, gamma and neutron attenuation capacities of boron-tellurite glass system utilizing Phy-X/PSD database, Mater. Chem. Phys. 274 (2021). https://doi.org/10.1016/j.matchemphys.2021.125166.

[10] H.A. Saudi, W.M. Abd-Allah, K.S. Shaaban, Investigation of gamma and neutron shielding parameters for borosilicate glasses doped europium oxide for the immobilization of radioactive waste, J. Mater. Sci. Mater. Electron. 31 (2020) 6963–6976. https://doi.org/10.1007/s10854-020-03261-6.

[11] RM El-Sharkawy., EA Allam**.,** Atef El-Taher., E.R Shaaban, and ME Mahmoud**.,** Synergistic Effect of Nano-bentonite and Nano cadmium Oxide Doping Concentrations on Assembly, Characterization and Enhanced Gamma-Rays Shielding Properties of Polypropylene Ternary Nanocomposites. International Journal of Energy Research. 45 (6), 8942-8959. 2021.

[12] Y. B, Saddeek., KH. S, Shaaban., R. Elsaman., A., El-Taher., T.Z Amer., Attenuation-density anomalous relationship of lead alkali borosilicate Glasses. Radiation Physics and Chemistry 150, 182–188. 2018

[12] ME Mahmoud., RM El-Sharkawy, EA Allam., R. Elsaman., Atef El-Taher., Fabrication and characterization of phosphotungstic acid-Copper oxide nanoparticles-Plastic waste nanocomposites for enhanced radiation-shielding. Journal of Alloys and Compounds 803, 768-777. 2019.

[14] S.R. Manohara, S.M. Hanagodimath, K.S. Thind, L. Gerward, On the effective atomic number and electron density: A comprehensive set of formulas for all types of materials and energies above 1 keV, Nucl. Instruments Methods Phys. Res. Sect. B Beam Interact. with Mater. Atoms. 266 (2008) 3906–3912. https://doi.org/10.1016/j.nimb.2008.06.034.

[15] R. Sharma, J.K. Sharma, T. Kaur, T. Singh, J. Sharma, P.S. Singh, Experimental investigation of effective atomic numbers for some binary alloys, Nucl. Eng. Technol. 49 (2017). https://doi.org/10.1016/j.net.2017.06.007.

[16] A. Kumar, A. Jain, M.I. Sayyed, F. Laariedh, K.A. Mahmoud, J. Nebhen, M.U. Khandaker, M.R.I. Faruque, Tailoring bismuth borate glasses incorporating PbO/GeO2 for protection against nuclear radiation, Sci. Rep. 11 (2021) 1–14. https://doi.org/10.1038/s41598-021-87256-1.

[17] Atef El-Taher., Hesham MH Zakaly., Mariia Pyshkina, EA Allam., R M El-Sharkawy, ME Mahmoud., Mohamed AE Abdel-Rahman., A comparative Study Between Fluka and Microshield Modelling Calculations to study the Radiation-Shielding of Nanoparticles and Plastic Waste Composites. Zeitschrift für anorganische und allgemeine Chemie 647 (10), 1083-1090. 202.

[18] A.U. Alam, The effects of oxygen plasma and humidity on surface roughness, water contact angle and hardness of silicon, silicon dioxide, and glass, (n.d.). https://doi.org/10.1088/0960-1317/24/3/035010.

[19] RM El-Sharkawy., EA Allam., Atef El-Taher., Reda Elsaman., EE Massoud., ME Mahmoud., Synergistic effects on gamma-ray shielding by novel light-weight nanocomposite materials of bentonite containing nano Bi2O3 additive. Ceramics International 48 (5), 7291-7303. 2022.

[20] I.I. Bashter, Calculation of radiation attenuation coefficients for shielding concretes, Ann. Nucl. Energy. 24 (1997) 1389–1401. https://doi.org/10.1016/S0306-4549(97)00003-0.

[21] P.P. Pawar, C.S. Mahajan, R.G.B. Arts, S.B.L. Commerce, R.B. Science, Measurement of mass and linear attenuation coefficients of gamma-rays of Glycine for, 3 (2013) 53–56.

[22] M.A.R. Alhammashi, H.D. ALattabi, M.J.R. Aldhuhaibat, Improving the attenuation Ability of gamma rays for silicate glass system composites (GS-PbO): A comparative theoretical study, IOP Conf. Ser. Mater. Sci. Eng. 928 (2020). https://doi.org/10.1088/1757-899X/928/7/072077.

[23] Atef El-Taher., AM Ali., YB Saddeek., R. Elsaman., H Algarni., KS Shaaban., T.Z Amer., Gamma-ray shielding and structural properties of iron alkali alumino-phosphate glasses modified by PbO. Radiation Physics and Chemistry, 165, 108403. 2019.

[24] RM El-Sharkawy, EA Allam, A. El-Taher, ER Shaaban, ME Mahmoud., Synergistic effect of nano-bentonite and Nano cadmium oxide doping concentrations on assembly, characterization, and enhanced gamma-rays shielding properties of polypropylene ternary nanocomposites. International Journal of Energy Research, 2021, 45 (6), 8942-8959

[25] H.A. Saudi, · Hossam, M. Gomaa, The effect of Nb 2 O 5 on fast neutron removal cross-section, optical, and structural properties of some calcium borate oxide glasses containing Bi 3+ ions, Radiat. Detect. Technol. Methods. 3 (2019) 7. https://doi.org/10.1007/s41605-018-0083-x.

[26] A.M. El-Khayatt, A. El-Sayed Abdo, MERCSF-N: A program for the calculation of fast neutron removal cross sections in composite shields, Ann. Nucl. Energy. 36 (2009) 832–836. https://doi.org/10.1016/j.anucene.2009.01.013.

[27] A.M. El-Khayatt, Calculation of fast neutron removal cross-sections for some compounds and materials, Ann. Nucl. Energy. 37 (2010) 218–222. https://doi.org/10.1016/j.anucene.2009.10.022.